THE JOURNAL OF PHYSICAL CHEMISTRY B

ARTICLE

pubs.acs.org/JPCB

Proton-Transfer Reaction Dynamics within the Human Serum Albumin Protein

Boiko Cohen, Cristina Martin Álvarez, Noemí Alarcos Carmona, Juan Angel Organero, and Abderrazzak Douhal*

Departamento de Química Física, Facultad de Ciencias Ambientales y Bioquímica, and INAMOL, Universidad de Castilla-La Mancha, Avenida Carlos III, S/N, 45071 Toledo, Spain

Supporting Information

ABSTRACT: We report on femto- to nanosecond studies of the excited state intermolecular proton transfer (ESPT) reaction of trisodium 8-hydroxypyrene-1,3,6-trisulfonate (pyranine, HPTS) with the human serum albumin (HSA) protein. The formed robust 1:1 complexes (K_{eq} = (2.6 ± 0.1) × 10^6 M^{-1}) show both photoacid (~430 nm) and conjugated photobase (~500 nm) emissions of the caged HPTS in its protonated structure. The proton-transfer reactions in these complexes proceed in a large time window, spanning from 150 fs to ~1.2 ns. The ultrafast component reflects a direct H-bond breaking and making in the robust complexes, involving the carboxylate groups of the amino acids, while the slowest one is arising from the slow dynamics of the so-called biological water. Additional time constants of the caged photoacid to give the conjugated photobase are observed, assigned to the ESPT reaction within "loose" complexes (3 to tens of picoseconds), and 130 ps and 1.2 ns due to the slow dynamics of the water molecules around the protein residues and involved in the proton transfer. The fs−ns anisotropy measurements confirm the robustness of the HPTS:HSA complexes. Our results indicate that, even though robust 1:1 complexes between HPTS and the HSA are formed, the system is heterogeneous, due to different possible interactions of the dye with the inside/outside parts of the protein. Furthermore, we find lower values of the initial anisotropy ($r(0)$) in the protein (0.33) and in γ-CD (0.28) in comparison with buffered aqueous solution (0.385). We propose that caging HPTS by the HSA protein and by the cyclodextrin affects the electronic redistribution in a different degree of mixing between the ^1L_a and ^1L_b states in the formed deprotonated form, for which the interactions of the sulfonate groups with the surroundings should play a key role.

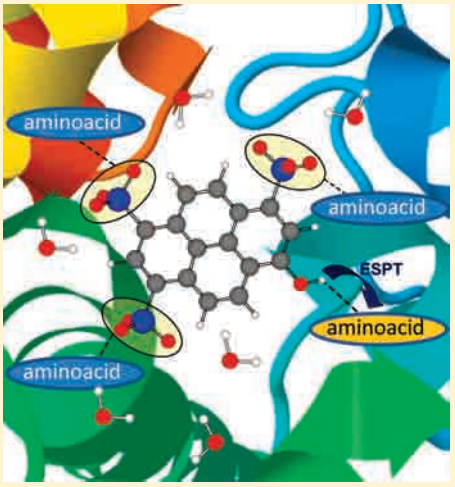

1. INTRODUCTION

Hydrogen bonds and related proton transfer reactions are one of the fundamental processes in chemistry and biology.[1] Since the seminal works of Weller and Eigen,[2−6] the mechanism of the acid−base reactions has drawn the attention of both experimentalists and theoreticians.[7−18] The Smoluchowski−Collins−Kimbal (SCK) model,[19,20] based on the spherically symmetric diffusion equation, has been used to describe this type of reactions.[21−23] In this model, the diffusion of the acid and the base through the solvent plays an important role, to bring the reactants to a well-defined distance, required for the reaction to take place at a certain rate. With the introduction of ultrafast time-resolved spectroscopy, it was made possible to study the elementary steps of the proton transfer reactions.[9,24−35] These studies have shown that the SCK does not provide the full description of the experimental data at all times.[29,30] Furthermore, a distribution of H-bonded reaction complexes with different numbers of bridging water molecules has been found and a branching out of the reaction pathways has been proposed, depending on the base concentration and stregth.[25−28,30] In this type of reactions, the solvent plays a crucial role through solvent fluctuations and reorganization and much effort has been put forth in order to understand its influence on the ESPT reaction. Depending on the strength of the H-bond, the type of acid and base, and on the strength of interaction with the solvent, nonadiabatic and adiabatic regimes of the PT have been identified.[13,15]

One of the widely used reporters in acid−base reactions that can undergo a photoinduced excited state intermolecular proton-transfer (ESPT) reaction is trisodium 8-hydroxypyrene-1,3,6-trisulfonate (pyranine, HPTS, Scheme 1).[10,36,37] HPTS belongs to a class of chemical compounds known as photoacids.[36] Upon excitation, its acidity changes significantly from pK_a^0 ~ 7.7 to pK_a^* ~ 0.6. The excited state behavior of HPTS in bulk water, in the presence of bases (with varying concentrations and strength) and in more complex environments (reverse micelles, cyclodextrins, ionic liquids, and

Received: January 11, 2011
Revised: February 24, 2011
Published: April 08, 2011

Scheme 1. Schematic Presentation of the Molecular Structure of Trisodium 8-Hydroxypyrene-1,3,6-trisulfonate (HPTS), the Human Serum Albumin (HSA) Protein, and γ-CD[a]

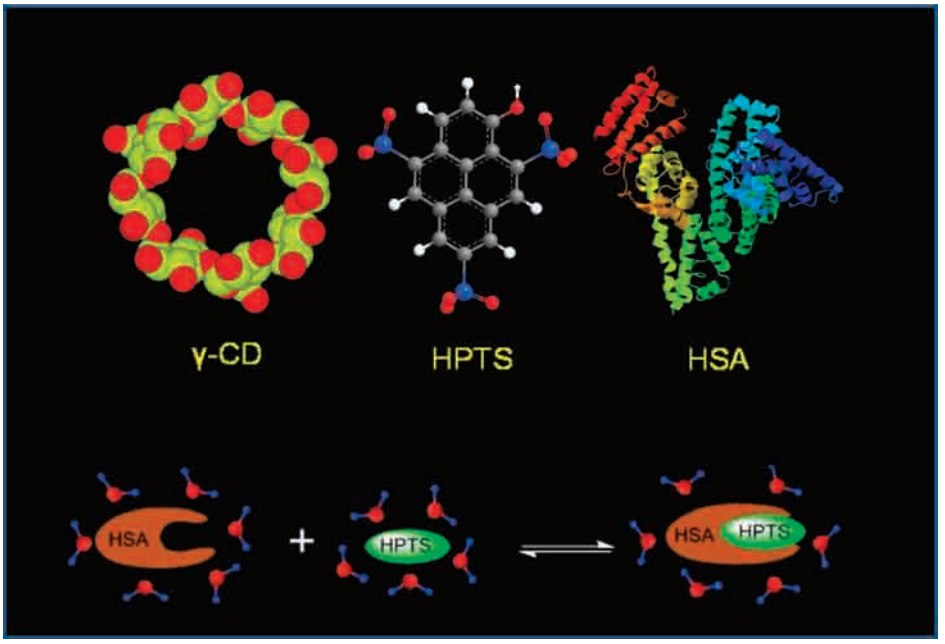

[a] The lower part shows an illustration of a protein−ligand recognition process. The represented structures are not to scale.

proteins), has been studied and explained using several kinetic models to describe the ESPT reaction.[38−48] The ESPT reaction in H_2O is characterized with a time constant of ∼90 ps, while that in D_2O proceeds in 220 ps, which gives a kinetic isotope effect of ∼2.4. Earlier studies on the nature of the electronic transitions in pyranine have identified two electronic states, ^1L_a and ^1L_b.[35,49] Many efforts have been put forth to describe these states and to characterize their role in the overall ESPT reaction.[35,37,50−52]

Human serum albumin (HSA, Scheme 1) protein is the most abundant blood plasma protein. It plays an important role in the transport and distribution of various complex chemical and biological systems, such as fatty acids, drugs, and steroid hormones.[53] The crystal structure of the HSA reveals three homologous domains referred to as I, II, and III that are a product of two subdomains, A and B, with common structural motifs.[53,54] The principal regions of ligand bindings to HSA are located in hydrophobic cavities in subdomains IIA (binding site I) and IIIA (binding site II). Furthermore, as suggested by crystal structure and drug binding studies, site I is dominated by the strong hydrophobic interactions with most neutral, bulky, heterocyclic compounds, whereas, with most aromatic carboxylic acids, binding site II mainly involves ion (dipole)−dipole, van der Waals, and/or hydrogen-bonding interactions in the polar cationic group of HSA.[53−55] The HSA protein undergoes reversible conformational transitions with changes in the pH. Using the femtosecond fluorescence up-conversion technique, the observed changes in the solvation dynamics were correlated with the pH induced change in the conformational structure of the protein.[56]

Here, we report on a study of the electronically excited HPTS in aqueous phosphate buffer solutions (pH 7), and in the presence of HSA protein. The results obtained in the bulk solution are in agreement with previous observations, involving low base concentrations.[25−28,30] In the presence of HSA protein, the dynamics of the ESPT reaction is more complex, indicating the heterogeneous nature of the system and revealing site specific interactions of the complex that lead both to speeding up and slowing down of the processes depending on the nature of the complexes. To the best of our knowledge, this is the first report on the femtosecond excited state dynamics of HPTS interacting with the HSA protein.

2. MATERIALS AND METHODS

Trisodium 8-hydroxypyrene-1,3,6-trisulfonate (pyranine, HPTS, Scheme 1, >98% pure, Fluka), human serum albumin (HSA) protein (Sigma-Aldrich, >97%, lyophilized powder), γ-cyclodextrin (γ-CD, Cyclolab, >99% pure), KH_2PO_4, and NaOH (Scharlab, > 98%) were used as received. Samples were prepared using deionized water. Potassium phosphate buffer (0.1 M at pH 7.0) was used in the preparation of the samples. Steady state absorption and emission spectra were recorded on Varian (Cary E1) and Perkin-Elmer (LS 50B) spectrophotometers, respectively. The concentration of HPTS was kept at $\sim 10^{-5}$ M, and that of the HSA protein was 5×10^{-5} M, unless stated otherwise. The samples for the femtosecond experiment were prepared to give an optical density of 0.5 in a 1 mm cell at the excitation wavelength.

The emission lifetimes were measured using a previously described time-correlated single-photon-counting picosecond spectrophotometer (FluoTime 200).[57] The sample was excited by a 40 ps pulsed (20 MHz) laser centered at 371, 393, or 430 nm, and the emission signal was collected at the magic angle (54.7°). The instrument response function (IRF) was typically 65 ps. The emission decays were convoluted to the IRF and fitted to a multiexponential function using the Fluofit package (Picoquant).

Femtosecond (fs) emission transients have been collected using the fluorescence up-conversion technique. The system consists of a femtosecond Ti:sapphire oscillator Mai Tai HP (Spectra Physics) coupled to second harmonic generation and up-conversion setups.[58] The oscillator pulses (90 fs, 2.5 W,

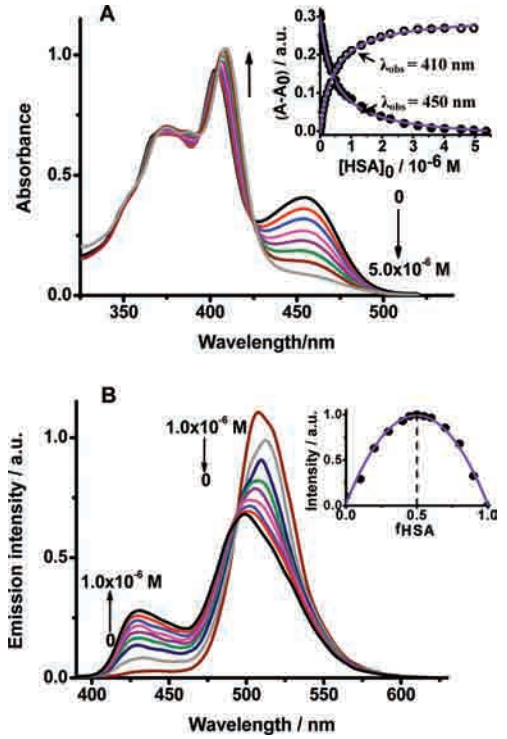

Figure 1. (A) UV−visible absorption spectra of HPTS in an aqueous phosphate buffer (pH 7) and in the presence of different concentrations of HSA $\{(0; 0.033; 0.133; 0.298; 0.495; 0.852; 1.64; 5) \times 10^{-6}$ M$\}$. The inset shows the change in the absorption intensity $(A - A_0)$ at 450 and 410 nm of the HPTS solution with the concentration of HSA. The solid line shows the best fit assuming a 1:1 HPTS/HSA complex using a model described in the text. (B) Emission spectra of HPTS in buffer (pH 7) and in the presence of different concentrations of HSA protein $\{(0; 0.017; 0.033; 0.05; 0.066; 0.1; 0.166; 0.331; 1) \times 10^{-6}$ M$\}$. The excitation wavelength was 380 nm. The inset shows a Job's plot of HPTS/HSA emission at 430 nm upon increasing the molar fraction of HSA (f_{HSA}) and upon excitation at 380 nm.

80 MHz) were centered at 780 or 880 nm and doubled in an optical setup through a 0.5 mm BBO crystal to generate a pumping beam at 390 or 440 nm (∼0.1 nJ). The polarization of the latter was set to the magic angle with respect to the fundamental beam. The sample has been placed in a 1 mm thick rotating cell. The fluorescence was focused with reflective optics into a 0.3 mm BBO crystal and gated with the fundamental fs beam. The IRF of the apparatus (measured as a Raman signal of pure solvent) was 170 fs (fwhm) for 390 and 440 nm excitation, respectively. To analyze the decays, a multiexponential function convoluted with the IRF was used to fit the experimental transients. All experiments were performed at 298 K.

The time-resolved anisotropy was constructed using the expression $r(t) = (I_{\parallel} - GI_{\perp})/(I_{\parallel} + 2GI_{\perp})$, where G is the ratio between the fluorescence intensity at parallel ($I_{\parallel}$) and perpendicular ($I_{\perp}$) polarizations of the emission with respect to the excitation beam. The value of G was measured at a gating window, in which the fluorescence is almost completely depolarized (tail-matching technique). The quality of the fits was characterized in terms of the residual distribution and reduced χ^2 values.

3. STEADY STATE OBSERVATIONS

To begin with, Figure 1A shows the ground state UV−visible absorption spectra of HPTS in pH 7 phosphate buffer aqueous solution, and in the presence of various concentrations of the HSA protein. In the buffer solution, the absorption intensity maximum is at 404 nm arising from the protonated form (ROH) of HPTS with an additional absorption with a maximum at 454 nm, assigned to the deprotonated form (RO^-). The latter is due to the presence of the phosphate ions, as it is not observed in pure neutral water.[42] The molar extinction coefficients of both the ROH and RO^- forms at their maximum intensity (404 and 454 nm, respectively) are 25000 and 20000 L mol^{-1} cm^{-1}. Upon addition of HSA, the S_0 equilibrium shifts toward the protonated form, and the band intensity at 454 nm decreases with the increase of the protein concentration. This change is concurrent with a red shift of ∼5 nm (∼300 cm^{-1}) to 409 nm due to an increase in the absorption band intensity of the ROH form interacting with the protein. This red shift is explained in terms of stronger H-bonding interactions of the ROH form with the amino acids of the protein than with water molecules (Scheme 2).

Scheme 2. Schematic Illustration of the Encapsulated HPTS Photoacid Form with the HSA Protein, Where Specific and non-Specific Interactions of the Amino Acids Play a Role in the Robustness and Dynamics of the Complex[a]

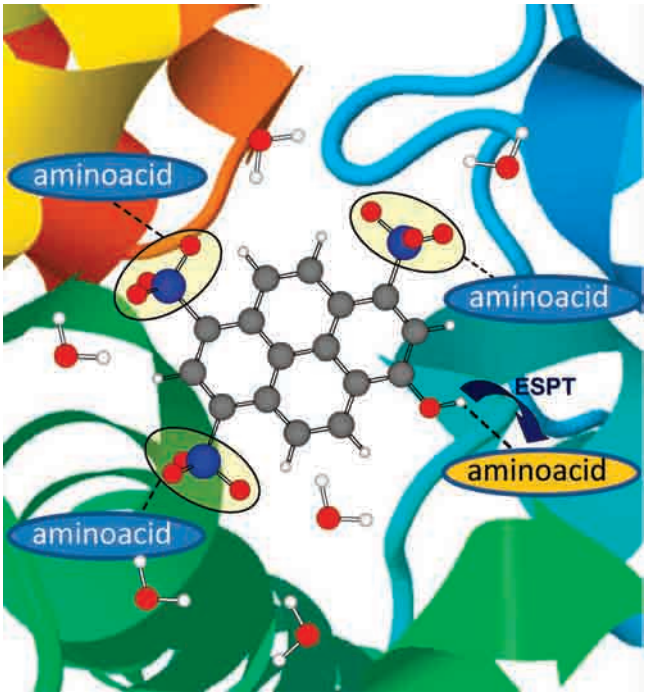

[a] The represented structures are not to scale.

Figure 1B shows the emission spectra of HPTS in the phosphate buffer and in the presence of different concentrations of the protein. To avoid the autoabsorption effect in the emission experiment, which may give some distortion of the 430 nm emission band, we used a sample of low optical density at 400 nm (0.038). The spectrum in the buffer solution has a very weak band at 437 nm (22883 cm^{-1}) from the ROH* form and a strong one from RO^-* at 508 nm (19685 cm^{-1}). In the presence of the protein, the band arising from the caged ROH* emission shifts (by 6 nm, ∼320 cm^{-1}) to lower wavelengths (431 nm, 23202 cm^{-1}), and the band due to the caged RO^-* emission shifts (by 9 nm, ∼360 cm^{-1}) to the blue from 508 to 499 nm (20040 cm^{-1}). Thus, an ESPT reaction is taking place in the HPTS:HSA complexes (Scheme 2). Both shifts to the

higher energy side indicate emissions from the complexes between HPTS and the HSA protein (431 and 499 nm). In addition to that, we still observe a red edge shoulder in the noncomplexed RO^{-*} emission band.

The Stokes shift of the free HPTS in phosphate buffer is ~1870 cm^{-1} (ROH) and 2342 cm^{-1} (RO^-), while for that complexed with the protein it is ~1250 cm^{-1} (ROH/HSA) and ~1700 cm^{-1} (RO^-/HSA). The decrease in the Stokes shift value (~630 cm^{-1}) upon interaction with the protein indicates a lower electronic redistribution in the caged HPTS or a destabilization of the excited species by 930 cm^{-1} as the bonded ROH is stabilized by 300 cm^{-1} (Figure 1) when compared with the one in the phosphate buffer. Furthermore, the effect of the interaction of the HPTS with the protein on both ROH and RO^- Stokes shifts is the same (~630 cm^{-1}), suggesting that such interactions are not significantly sensitive to the new electronic distribution in the RO^- due to the ESPT reaction. In addition to that, there is a new shoulder in the emission band in the presence of the protein, shifted to the red and which is due to a more hydrophobic environment that affects the emission of this deprotonated form. A similar band has been found in the emission spectra of HPTS interacting with γ-CD, where the additional amino acid residues of the protein are not present, and which was assigned to the conjugated photobase, trapped in the cavity.[42,48]

The excitation spectrum collected at 430 nm emission has a maximum of intensity at 404 nm, which coincides with the absorption maximum of the ROH (Figure 1, Supporting Information), while that obtained at 510 nm emission shows an additional band at 455 nm, assigned to the RO^- formed at S_0. In the presence of HSA, the excitation spectrum of the interacting ROH has a maximum of intensity at 409 nm in agreement with the absorption changes shown in Figure 1. The intensity of the RO^-, being weaker with comparison to the corresponding intensity observed in bulk water, suggests that there is still existence of free dye in the presence of the HSA protein.

To determine the binding constant between HPTS, the protein, and the complexes, we used eqs 1−7, which assume a 1:1 stoichiometry of the complexes. We took into consideration the fact that the host (HSA) is not in very large excess compared to the guest (HPTS). The equilibrium constant is expressed by the following equation:

$$K_{eq} = \frac{[\text{HPTS:HSA}]}{[\text{HPTS}][\text{HSA}]} \tag{1}$$

The concentrations of free HPTS and HSA can be described by

$$[\text{HPTS}] = [\text{HPTS}]_T - [\text{HPTS:HSA}] \tag{2}$$

$$[\text{HSA}] = [\text{HSA}]_T - [\text{HPTS:HSA}] \tag{3}$$

where $[\text{HPTS}]_T$ and $[\text{HSA}]_T$ are the total concentrations of HPTS and HSA, respectively. The concentration of the complex is given by

$$[\text{HPTS:HSA}] = \frac{1}{2}[([\text{HPTS}]_T + [\text{HSA}]_T + K_{eq}^{-1}) \pm \sqrt{([\text{HPTS}]_T + [\text{HSA}]_T + K_{eq}^{-1})^2 - (4[\text{HPTS}]_T[\text{HSA}]_T)}] \tag{4}$$

The following equations relate the absorbance measurements of the bimolecular equilibrium:

$$\frac{A_i}{A_S} = \frac{[\text{HPTS:HSA}]_i}{[\text{HPTS:HSA}]_S} = \frac{[\text{HPTS:HSA}]}{[\text{HPTS}]_T} \tag{5}$$

$$A_i = \frac{A_S[\text{HPTS:HSA}]}{[\text{HPTS}]_T} \tag{6}$$

where A_i is the absorbance change of HPTS produced by the binding of increasing quantities (i) of HSA, A_S is the absorbance change of HPTS at saturation. $[\text{HPTS:HSA}]_i$ is the concentration of the complex as varying quantities (i) of HSA are added to a constant amount of HPTS, and $[\text{HPTS:HSA}]_S$ is the concentration of the complex at saturation of HSA. Substituting eq 4 into eq 6 yields the final equation:

$$A_i = \frac{1}{2[\text{HPTS}]_T}\{A_S[(K^{-1} + [\text{HPTS}]_T + [\text{HSA}]_T) - \sqrt{([\text{HPTS}_T] + [\text{HSA}]_T + K_{eq}^{-1})^2 - (4[\text{HPTS}]_T[\text{HSA}]_T)}]\} \tag{7}$$

The best fit (R^2 = 0.9978, n = 26) gives $K_{eq} = (2.6 \pm 0.1) \times 10^6$ M^{-1} and $\Delta G^0 = -8.74 \pm 0.08$ kcal/mol at 298 K. To further confirm the 1:1 stoichiometry of the complexes, we used the Job's plot technique and analyzed the change in the fluorescence intensity of the complex (ROH:HSA) at 430 nm versus the molar fraction of the protein (f_{HSA}) in the used solutions (inset of Figure 1B). The maximum in the fluorescence intensity in the plot occurs at f_{HSA} = 0.5 and clearly indicates that the complexes have a 1:1 stoichiometry.

4. EXCITED STATE BEHAVIOR

4.1. Picosecond Observation in Buffered Aqueous Solution and in the HSA Protein. To get information on the ns−ps behavior of the excited structures, Figure 2A shows the time-resolved emission spectra (TRES) of the free HPTS in a phosphate buffer (pH 7), upon excitation at 371 nm. Figure 2 in the Supporting Information shows the emission decays at two selected wavelengths of observation, corresponding to the signals of ROH* and RO^{-*}. Table 1 gives the obtained values from the multiexponential fits. At the blue edge of the emission spectra, where we mainly monitor the ROH* emission, the time evolution of the spectra was fit by a three-exponential function with time constants of 95 ps, 260 ps, and 5.3 ns. The short time component has a pre-exponential factor of 90% at 450 nm, and it decreases to 65% at 480 nm. The pre-exponential factor of the 260 ps component has a value between 10 and 15%, while that of the 5.3 ns component is ~1% at 450 nm, and it increases with wavelength to 22% at 480 nm. When gating at the red side of the spectra (the RO^{-*} emission), the transients are fit by a biexponential function giving two time constants: a rise of ~100 ps and a decay of ~5.3 ns (Table 1). The rise time corresponds to the decay of the ROH* form monitored at the blue part (450−480 nm). Similar values in water were reported and assigned to the ESPT reaction of ROH* with water molecules leading to RO^{-*}. We adopt the same conclusion. We assign the 260 ps blue component to the lifetime of the ROH* structure and the 5.3 ns one to the fluorescence lifetime of the RO^{-*}. Thus, the 260 ps component is shorter than the reported one in normal bulk water (~5 ns), and the difference is due to the presence of phosphate anions that affect its fluorescence

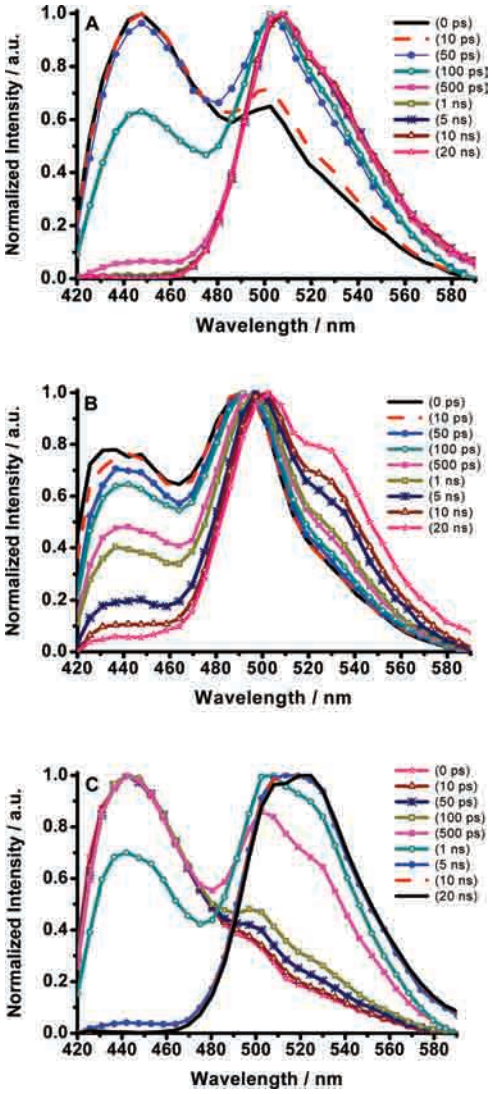

Figure 2. Normalized (to the maximum of intensity) magic-angle time-resolved emission spectra of HPTS in (A) phosphate buffer at pH 7, (B) phosphate buffer in the presence of 10^{-6} M HSA, and (C) phosphate buffer in the presence of 4×10^{-3} M γ-CD, gated at the indicated delay times after excitation at 371 nm. The inset gives the gating times of the spectra.

lifetime.[16,59] We did not find any evidence for geminate recombination leading to the back ESPT in contrast to the situation in pure water.[16−18,60] This is due to the presence of the phosphate anion in the buffer solution. Previously, it was shown that small amounts of base in low concentrations in the aqueous solutions can affect the geminate recombination by acting as scavengers for the ejected protons, without directly influencing the rate of the proton transfer reaction.[33,59] The TRES clearly show the absence of an excited state equilibrium between the ROH* and RO^-* forms, as the emission of the former vanishes at ∼260 ps, while that of the latter remains.

In the presence of the HSA protein, the TRES and the corresponding emission decays (Figure 2, Supporting Information) reveal more complex dynamics (Figure 2B). The spectra collected at the ROH* emission band (450−475 nm) decay multiexponentially, with time constants of 132 ps, 1.22 ns, and ∼4 ns (Table 2 and Figure 2B). The contribution of the ps component decreases, when we gate at longer wavelengths, and disappears at 490 nm, while the one of the 4 ns component increases with the

Table 1. Values of Time Constants (τ_i) and Normalized (to 100) pre-Exponential Factors (a_i) of the Multiexponential Functions Used in Fitting the ps Emission Transients of HPTS in Buffer at Different Wavelengths of Observation (λ_{em}) after ps Excitation at 371 nm[a]

λ_{em} (nm)	τ_1 (ps)	A_1 (%)	C_1 (%)	τ_2 (ps)	A_2 (%)	C_2 (%)	τ_3 (ns)	A_3 (%)	C_3 (%)
450	96	89	68	260	10.6	22	5.28	0.3	10
460	94	86	53	245	13	20	5.19	1	27
470	93	83	20	252	12	8	5.29	5	72
480	87	65	4	244	13	3	5.29	22	93
495	125	(-)7	0.2				5.28	93	99.8
510	118	(-)32	1				5.30	68	99
530	110	(-)37	1				5.30	63	99
550	114	(-)38	1				5.30	62	99
570	103	(-)40	1				5.30	60	99

[a] A negative sign indicates a rise component in the transient.

Table 2. Values of Time Constants (τ_i) and Normalized (to 100) pre-Exponential Factors (a_i) of the multi-Exponential Functions Used in Fitting the ps Emission Transients of HPTS Interacting with HSA at Different Wavelengths of Observation (λ_{em}) Excitation at 371 nm[a]

λ_{em} (nm)	τ_1 (ps)	A_1 (%)	C_1 (%)	τ_2 (ps)	A_2 (%)	C_2 (%)	τ_3 (ns)	A_3 (%)	C_3 (%)
420	132	42	4	1.22	25	19	3.60	33	77
435	132	44	4	1.22	22	17	3.67	34	79
480	132	25	1	1.22	14	10	4.69	51	61
510	132	(-)16	<1	1.22	(-)3	1	5.21	81	99
530	132	(-)16	1	1.22	(-)10	3	5.48	74	96
560	132	(-)18	1	1.22	(-)11	3	5.57	71	96

[a] A negative sign indicates a rise component in the transient.

observation wavelength up to 86% at 490 nm. The 1.2 ns component also disappears at 490 nm. The lack of rising components at 490 nm and the significant decrease in the pre-exponential factors of the two faster decay components (132 ps and 1.22 ns) indicate the presence of processes that are faster than the time resolution of the TCSPC system (IRF ∼ 65 ps). The spectral behavior of the blue-green emission (490−560 nm) is rather complex, and suggests contributions from at least three species, giving spectra with maxima at 490 nm (caged conjugated photobase) at shorter times (∼100 ps) and 510 nm (free RO^-*) at longer times (∼1 ns) and a shoulder at 535 nm at longer times (>1 ns), assigned also to differently caged RO^-*. This latter emission is very similar to the observed one for the caged deprotonated form in the γ-CD (Figure 2C and Figure 3 of the Supporting Information), which is in good agreement with a recent report.[42] The fit of the decays using a multiexponential function gives two rising components (132 ps and 1.22 ns) that correspond to the decays found at the blue side and a decaying component of 5.6 ns. A 300 ps time constant for the proton transfer of HPTS interacting with bovine serum albumin (BSA) protein has been reported.[47] Furthermore, the ESPT reaction taking place inside a protein pocket should be affected by the change in the dynamical properties of the water molecules in the protein (biological water).[47,61,62] It should be noted that proton-transfer (PT) reactions do not proceed in the same way inside a protein and on its surface and the protein should not be treated as a homogeneous system.[63−65] Several experimental and theoretical studies on the ESPT reaction at a protein surface have suggested that residues at the protein surface could form proton-attractive domains and

share the proton among them at a very fast rate and, hence, generate transient situations in which the residues are getting sufficiently close to allow a proton transfer over a short distance. Furthermore, the passage of the proton should be accelerated by the electrostatic potentials that bias the diffusion of the proton between the donor−acceptor sites.[63−65] Inside the protein pockets, the water molecules are confined and the encapsulated dye will be subjected to specific and nonspecific interactions with the amino acid residues of the protein that will affect the rate of the PT reactions.[66] In addition, the local dielectric properties of the protein are inhomogeneous, and strongly dependent on the local chemical environment.[67] For example, in studies of the effect of the reorganization of protein polar groups on charge−charge interaction and the corresponding effective dielectric constant, it was reported that the dielectric constant for the interaction between ionizable groups in proteins is very different from the effective dielectric constant that determines the free energy of ion pairs in protein, and hence, one should consider the protein relaxation microscopically.[68,69]

A recent study on the ESPT of HPTS in γ-cyclodextrin (γ-CD) has found that the proton transfer process is slowed down with time constants of 140 ps and 1.4 ns, as a result of the confinement effect of the γ-CD.[42] Later, it was argued that the observed effect was rather due to the change in the properties of the water around the gates of the γ-CD cavity.[48] To further confirm the assignment of the 1.2 ns component in the presence of HSA, we recorded the TRES of HPTS in the presence of γ-CD (Figure 2C). The results clearly indicate that the band at 560 nm is arising from a slow ESPT reaction in the encapsulated HPTS: 1.2 and 1.4 ns in the presence of HSA protein and γ-CD, respectively. Notice also the same spectral position of these emissions, indicating little interaction of the conjugated photobase with the amino acid residues of the protein, and thus, the ESPT reaction in the caged ROH is taking place with the bound water molecules to the protein/γ-CD. We suggest a heterogeneity of the 1:1 complexes with the protein: a population having a strong docking of the dye and another in which the dye is exposed to the biological water molecules.

4.2. Femtosecond Interactions with Buffered Aqueous Solutions and the HSA Protein. To get information on the ESPT reaction and the involved processes, we interrogated the photoacid and its conjugated photobase emissions at the femtosecond time scale with a time resolution of ∼50 fs. Figure 3A shows the obtained transients at several wavelengths of observation. Figure 4A of the Supporting Information exhibits a short time window presentation of the gated signals. Table 3 gives the obtained time constants and pre-exponential factors, using a multiexponential fit. The signal at 420 nm decays multiexponentially to a constant offset (3.0 ns, 2%), with time constants of 0.43 ps (40%), 2.7 ps (25%), and 110 ps (33%). These times match to the rising components at 510 nm. The values of the short time constants of ∼0.45 and ∼3 ps are comparable to those reported for the primary steps of the ESPT reaction between HPTS and water molecules, and that involve ultrafast solvent response to the electronic excitation, leading to the locally excited state (0.3−1 ps),[24,33,34,49] charge redistribution, and slow solvent vibrational relaxation (2−3 ps).[33,34,37,49] The 110 ps time constant is due to the ESPT process from ROH* to produce RO^-*. Recent studies of the ESPT reaction between HPTS and several model bases such as acetates and chloroacetates in water, using femtosecond visible and infrared absorption spectroscopy, showed that there exists a distribution of H-bonded complexes that differ in the number of water molecules separating the dye

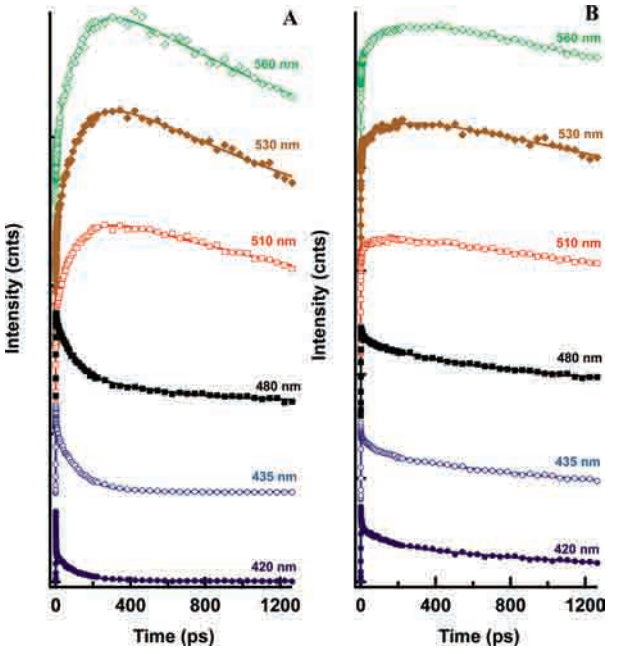

Figure 3. Femtosecond fluorescence up-conversion transients of HPTS (A) in phosphate buffer at pH 7 and (B) in the presence of 10^{-5} M HSA protein. The decays are gated at the indicated wavelengths. The fluorescence transients were vertically offset for a better representation. The short time window (0−2 ps) is given in Figure 4 of the Supporting Information. The excitation wavelength was 390 nm. The IRF (∼170 fs) was recorded as the Raman signal of water when gating at 440 nm. The solid lines represent the multiexponential fits following the model described in the text.

molecules and the base, and the proton is transferred via a relay mechanism.[25−31] At high base concentrations (>0.3−0.5 M) of acetate and choroacetate, for example, it was shown experimentally that the reaction is significantly faster and is the dominant reaction pathway.[25,30,33] At low base concentrations (<0.3 M), it was suggested that the proton-transfer reaction may proceed through several relevant pathways that involve direct proton transfer from ROH* to the base, or a competing transfer to water molecules and consecutive scavenging by the base.[25−28,30] The effectiveness of each pathway should then depend on the strength of the base and its concentration. When intimate information about the various reaction pathways is available, in this type of processes, the overall reaction dynamics is best described by a set of coupled rate equations.[27,28] When such information is not readily obtainable, it was suggested that the time-dependent SCK approach (see the Introduction) can provide a useful approximation about the reaction dynamics.[70,71] Under our experimental conditions, the phosphate ion concentration is low (0.1 M) and thus they cannot effectively attack the excited ROH* form to directly affect the rate of the proton transfer. Thus, we suggest a mechanism involving water molecule assisted proton transfer from the pyranine to the phosphate base present in the buffer solution.

To gain better information on the excited state dynamics of the free deprotonated HPTS in phosphate buffer at pH 7, we monitored the fluorescence up-conversion transients (Figure 5, Supporting Information) following a direct excitation of the ground state RO^- (λ_{ex} = 440 nm). The signal at 480 nm decays biexponentially, and the fit gives time constants of 0.75 ps (66%) and 2.4 ps (12%), in addition to a constant offset with a time constant of 5 ns due to the lifetime of the RO^-*, while at the red

Table 3. Values of the Time Constants (τ_i) and Normalized (to 100) pre-Exponential Factors (a_i) of the multi-Exponential Function Fitting the fs Emission Transients of HPTS in Phosphate Buffer at pH 7 and in the Presence of 10^{-5} M of HSA Protein[a]

	buffer, pH 7								HSA							
λ_{ex} = 390 nm	τ_1 (ps)	a_1 (%)	τ_2 (ps)	a_2 (%)	τ_3 (ps)	a_3 (%)	τ_4[b] (ns)	a_4 (%)	τ_1 (ps)	a_1 (%)	τ_2 (ps)	a_2 (%)	τ_3[b] (ps)	a_3 (%)	τ_4[b] (ns)	a_4 (%)
420 nm	0.43	40	2.7	25	110	33	3.0	2	0.20	18	3.9	16	250	19	3.0	47
435 nm	0.45	9	3.1	18	115	72	3.0	1	0.12	28	2.3	3	250	16	3.0	53
480 nm			3.3	3	106	57	5.0	40			13.3	10	250	15	5.0	75
510 nm	0.47	(-)6	2.9	(-)5	105	29	5.0	60	0.25	(-)8	9.2	(-)7	250	(-)11	5.0	74
530 nm	0.51	(-)7	3.1	(-)5	115	32	5.0	58	0.14	(-)13	5.7	(-)7	250	(-)21	5.0	59
560 nm	0.42	(-)6	3.2	(-)6	115	33	5.0	55	0.32	(-)10	7.2	(-)7	250	(-)20	5.0	63

[a] The excitation wavelength was 390 nm. A negative sign indicates a rising component. [b] Fixed mean lifetime values from the TCSPC measurements.

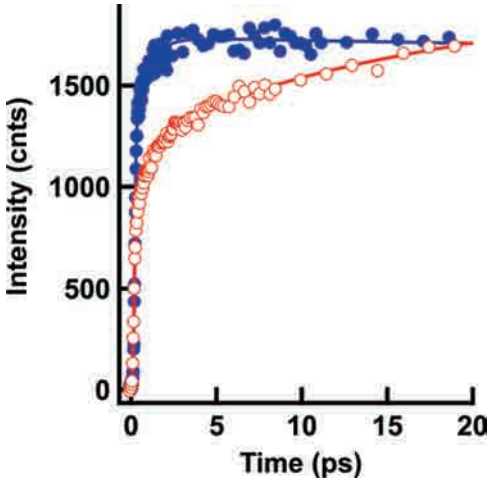

Figure 4. Femtosecond fluorescence up-conversion transients of HPTS in phosphate buffer gated at 530 nm, following an excitation at 440 nm (full circles) or at 390 nm (open circles). The solid lines represent the multiexponential fits following the model described in the text.

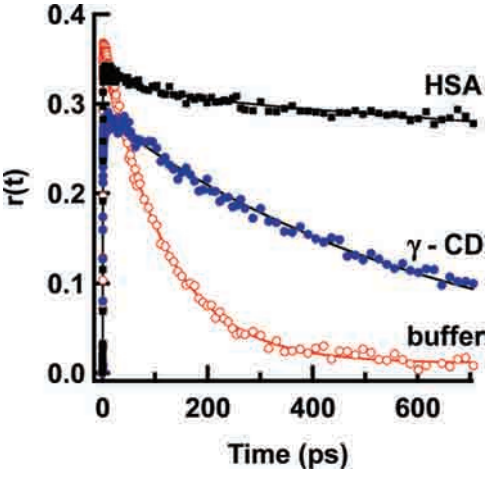

Figure 5. Femtosecond emission anisotropy of HPTS in phosphate buffer, in the presence of 10^{-5} M HSA protein and in the presence of ~10^{-3} M γ-CD. The excitation wavelength was 390 nm, and the emission was gated at 500 nm (buffer and the HSA protein) and 510 nm (γ-CD). The solid lines represent the fit using a single exponential function as discussed in the text.

edge of the deprotonated form emission band (530 nm), the fit gives a single rising component of 0.6 ps, similar to the decay component found at 480 nm. This time constant is due to an ultrafast electronic redistribution in the excited conjugated photobase and solvent response, while the second component of 2.6 ps is due to vibrational relaxation/cooling. At 505 nm, both the rising and the decaying components are overlapping; hence, we see only contribution from the 2.1 ps time constant, in addition to the long, 5 ns, one. Figure 4 illustrates the contribution of the 0.6 component in the ultrafast dynamics of the RO^{-}* (gated at 530 nm) independently on the type of its photogeneration—either upon direct excitation (440 nm) or following ESPT reaction in the ROH* form (λ_{ex} = 390 nm).

To get information on the ultrafast dynamics of the ESPT reaction within the HPTS:HSA complexes (Scheme 2), we performed fs emission experiments at different observation wavelengths spanning the caged ROH* and RO^{-}* emissions. Figure 3B shows the fluorescence up-conversion transients of HPTS in the presence of 10^{-5} M HSA protein in pH 7 phosphate buffer solution. Figure 4B in the Supporting Information exhibits the decays in a short delay time window (0−2 ps). Table 3 contains the values of the obtained time constants and pre-exponential factors fitting the transients. At 420 nm, the decay is multiexponential with time constants of 0.2 ps (18%), 3.9 ps (16%), 250 ps (19%). and 3.0 ns (47%). At the red side of the emission spectra, we find three rising components with time constants of 0.15 ps (13%), 5.7 ps (7%), and 250 ps (21%), in addition to a decaying one with a value of ~5 ns (59%). The 250 ps and 3−5 ns components at the blue and red part of the spectrum are the mean values of the time constants derived from the TCSPC measurements, and the nature of the assigned processes was discussed earlier. The short one, with a time constant of ~0.2 ps, corresponds to the ultrafast decay at the photoacid emission band (420 nm). This ultrafast component is much shorter than the one found for the free HPTS in phosphate buffer solution (0.45 ps) and the reported value in water (0.3−0.7 ps). On the other hand, its value is similar to the one reported for the direct acid−base irreversible reaction between pyranine and acetate base (0.15 fs).[25,29,32,33]

Several studies on the interaction between HPTS and carboxylate bases have reported that the initial step in the direct acid−base ESPT reaction proceeds within the instrument response and involves a tight complex between the proton donor and acceptor, such that the water molecules do not play a significant role in the reaction pathway. We explain our result with a direct interaction of the encapsulated dye with the amino acid residues of the protein that lead to an ESPT reaction (Scheme 2). Notice that the decrease of the emission Stokes shifts (350 cm^{-1}) suggests an energetic destabilization of the trapped and excited photoacid/conjugated photobase within the protein, most probably due to the interaction of the SO_3^{-} groups of HPTS with the protein (Scheme 2). On the basis of the nature

(ionic) of the molecular structure of the dye, we do not expect a significant contribution of hydrophobic interaction in the stabilization of the complexes (Scheme 1). In addition to that, following previous studies on the binding of several charged and neutral ligands, we suggest that the HPTS is mainly located within binding site II (subdomain IIIA) that is governed by dipole−dipole, van der Waals, and H-bonding interactions.[54,55,72−76] An X-ray structure study of salts composed of amino acids (similar to those of HSA protein) and negatively charged sulfonated aromatic dyes has found short (<3 Å) intermolecular H-bonds between the sulfonate groups of the dye and the neighboring amino acids.[77] This type of interactions should make robust complexes with an anionic character, as found for comparable systems.[55,78] This is in agreement with the ps anisotropy measurements (vide infra), where we found that the pyranine is deeply embedded inside the protein pocket, thus providing the conditions for a direct acid−base reaction with the amino acid residues inside the protein. In the anisotropy part, we will discuss the possible electronic polarization changes due to these interactions. Furthermore, in a study of the interaction of HPTS with the BSA protein, the possibility of an interaction between the excited pyranine with a carboxylate group from the protein binding site was considered.[47] The main conclusion was that, if such a group is present in the binding site, the reaction should proceed in a similar fashion as the direct acid−base irreversible proton transfer occurring at high base concentrations. In addition to that, in a study of the ESPT reaction between HPTS and ionic liquid based Triton-X (TX-100) micelles, it was shown that the pyranine binds to the interface of the micelle and participates in a direct reaction with the oxygen atoms of the TX-100. The reported time constants for this ESPT reaction were 0.3, 14, and 375 ps.[46] The value of 0.2 ps in the HPTS/HSA protein complex (Scheme 2) is similar to the reported (0.15 ps) one for the tight complexes in direct acid−base ESPT reactions.[28,30] However, it should be noted that for the protein solution there still exists a population of free dyes (∼9%) as calculated from the binding constant that might influence the value of the ultrafast time constant.

The intermediate component of ∼3 ps (420 and 435 nm) at the blue side of the spectrum becomes longer at the red side (480−560 nm) and has a value that ranges between 5 and 13 ps, depending on the wavelength of observation (Table 3). This behavior is explained in terms of the involvement of several parallel ESPT reactions, and it reflects the heterogeneity of the system (different interaction of HPTS with the amino acids as a result of different penetration within the protein). For the acid−base reactions in bulk aqueous solutions, the time constant of this component has been reported between 1.5 ps and tens of picoseconds.[9,25−30,32,33,79] The inconsistency of the values was assigned to an ESPT reaction in HPTS−base "loose" complexes, and it was modeled as distinct solvent-separated subpopulations.[25−28,79] Recently, a 5 ps component has been reported for the intrinsic tryptophan residue (W214) inside the hydrophobic pocket of the HSA protein.[56] The component was assigned to the initial solvation dynamics of the tryptophan residue, as a result of the local librational/rotational motions of trapped water molecules. An X-ray crystal structure study suggested that eight water molecules are in proximity (∼7 Å) of the indole ring of W214.[80] However, it should be noted that in aqueous solution the trapped water molecules are in fast dynamic exchange.[56,81] Thus, in similarity with the ultrafast component, the value of the intermediate ps component will be influenced by the contribution of the ps component of the free dye and the distribution of various acid−base pairs. Due to the proximity of the monitored time constants and the heterogeneity/complexity of the system, a precise assessment of their values is not possible.

4.3. Transient Anisotropy in Buffer, γ-CD, and HSA Protein. The time-resolved anisotropy ($r(t)$) decay in pure water (at 510 nm after excitation at 430 nm) fits to a single-exponential function giving $\varphi = 120 \pm 10$ ps (Figure 6, Supporting Information). Modeling HPTS as an oblate ellipsoid, we got a rotational relaxation time of 83 and 13 ps under stick-and-slip boundary condition limits, respectively.[82] This result shows the existence of strong H-bonding interactions between HPTS and the surrounding water molecules. In the presence of HSA protein, the anisotropy decay at 510 nm following an excitation at 430 nm shows a biexponential behavior, giving $\varphi_1 = 110 \pm 10$ ps and $\varphi_2 = 36 \pm 4$ ns, which correspond to the rotational time of the free molecule in water and to the global motion of HSA protein containing the dye, respectively. The reported values for the global Brownian rotation of the HSA protein are between 22 and 45 ns.[83,84] This result clearly indicates the robustness of the 1:1 complex between the dye and the protein in agreement with the large equilibrium constant ($2.6 \times 10^6\ M^{-1}$). However, due to the heterogeneity of the system, as a result of the presence of several accessible binding sites in the protein, we cannot exclude the existence of a small population of HPTS molecules bound to the protein surface or subpopulations of various complex configurations, due to the different extent of docking inside the protein pocket. A recent study on the ultrafast solvation dynamics of the HSA has reported on a large flexibility of the protein binding pockets, hence further enhancing the heterogeneous behavior of the system.[56]

Figure 5 shows the fs-resolved anisotropy decays following an excitation at 390 nm of HPTS in buffer (λ_{em} = 500 nm) and in the presence of the HSA protein (λ_{em} = 500 nm) and γ-CD (λ_{em} = 510 nm). In buffer, we find a monoexponential decay with a time constant of 115 ± 10 ps. This value is in agreement with previously published data for the rotational time of HPTS in bulk water (140 ps).[46] The initial anisotropy ($r_0 = 0.385$) is close to the ideal one (0.4) and corresponds to an angle of ∼13° between the absorption and emission transition moments.

In the presence of the protein, we find a biexponential decay with a small contribution (∼10%) from the fast (∼150 ps) component, arising from the minor population of free dye, and a long component (∼90%) resolved in the ps measurements to give a time constant of 36 ns. This time is comparable to that of the global motion of the protein, indicating a robust complex between the dye and the protein.[83,84] The initial anisotropy ($r(0)$) decreases only slightly from 0.385 in buffer to 0.33 in the presence of the protein. This value corresponds to ∼20° between the absorption and emission transient moments. Encapsulation by γ-CD further decreases the value of the initial anisotropy to 0.28 ($\alpha = 27°$) and the anisotropy decay is monoexponential with a time constant of ∼0.7 ns, which is in agreement with previous observations.[42] Using the hydrodynamic theory, the value of 0.7 ps gives a length of the 1:1 γ-CD/HPTS complex of ∼15 Å (viscosity, η = 1.13 mPa·s; volume, V = 2620 Å^3; and T = 293 K).[42] This value indicates that the part (∼7 Å) of the molecule containing the OH and the SO_3^- at position 6 is projected outside the γ-CD cavity, while the other part, containing the sulfonate groups at positions 1 and 3, is encapsulated. This is in agreement with previous studies on the proton antenna effect of the γ-CD outer surface.[48] Earlier reports on the nature of the electronic transitions in pyranine have identified two electronic states, ^1L_a and ^1L_b.[35,50] A three-state model has been suggested for the ESPT

reaction that involves ^1L_b to ^1L_a state inversion. However, in recent works, it was shown by magnetic circular dichroism, Stark, and polarization spectroscopy that there is a strong mixing between the two states and that the lowest excited state in both the protonated and deprotonated forms of HPTS is the ^1L_a state; the state inversion mechanism was ruled out.[50,51] Furthermore, it was found that the hydrogen bonding ability and the polarity of the solvent can influence to a certain extent the mixing between the two states.[50] The most probable reason for this effect was suggested to be due to the H-bonding interaction between the solvent and the three sulfonate groups.[50,52] Even though some uncertainty persists on the involvement of the ^1L_b, the general agreement is that the ESPT reaction and the emission proceed from the lower energy ^1L_a state.[35,50,52]

In light of these reports and the present one, we believe that the values of the initial anisotropy in the caged conjugated photobase reflect a change in the mixing between the two lowest electronic states as a result of the change in the electronic redistribution in HPTS, due to different interactions with its surrounding. Conversely, we cannot exclude the possibility of a ^1L_b to ^1L_a state inversion, as it was suggested that such a process should proceed at time scales faster than 100 fs.[52] As described earlier, in the protein environment, the molecule forms a robust complex and interacts with the amino acid residues. It is possible that such interactions might change the electronic part of the wave function that will induce a change in the transient dipole moments of ROH and/or RO^- emission, which in turn will provoke an inhomogeneous broadening of the emission transition dipole moment, even at a selected wavelength of observation. However, these interactions might have opposite effects on the electronic redistribution. On one hand, HPTS is bonded through its sulfonate groups to the amino acid residues, and on the other hand, it forms H-bonds with the residues through the hydroxyl group (Scheme 2). As a result, only a minor decrease in the value of the initial anisotropy is observed (from 0.385 in buffer to 0.33 in the presence of the HSA protein). This high initial anisotropy value points toward strong guest:host electrostatic and H-bonding interactions and hindrance of any rotational diffusion of the encapsulated ligand (HPTS), as observed for systems with excited state intramolecular proton transfer reactions.[55] It should be noted also that the intrinsic experimental fluorescence detection configuration with parabolic focusing mirrors leads to some mixing of polarization. The robustness of the complex is further confirmed by the lack of any initial ultrafast components. The large and constant anisotropy on the longer time scale (up to 700 ps) confirms the absence of diffusive motion of the dye in the protein pocket. In the case of γ-CD, the value of $r(0)$ is lowered further, 0.28, since only the interaction between the OH group of the pyranine with the water molecules found at the gate of the γ-CD cavity is present, in addition to the nanoconfinement effect of the cage. This is in agreement with the proton antenna effect model of the γ-CD outer surface, where it was suggested that the PT reaction proceeds to the solvent rather than to the confined inner volume.[48] Thus, the local environment of the guest trapped inside the CD is different from the one found in the protein, which will lead to a different $^1L_a/^1L_b$ mixing and different electronic redistribution. This explanation is in agreement with the red-shifted emission of the RO^{-}* complexes, involving γ-CD (530 nm) compared to that of the protein (490 nm).

5. CONCLUSION

We have studied the ESPT reaction of HPTS in phosphate buffer at pH 7 and in the presence of the HSA protein, using steady state and the femtosecond to nanosecond fluorescence techniques. Contrary to the situation in pure water, in the phosphate buffer, we found ground state equilibrium between the photoacid and its conjugated photobase due to the presence of the phosphate ions. Addition of the protein leads to the formation of a robust 1:1 inclusion complex with the ROH form of HPTS.

The complexes show both photoacid and RO^{-}* emissions due to the interactions of the trapped ROH* forms with the amino acid residues of the protein. The time-resolved emission spectra clearly indicate the formation of different 1:1 inclusion complexes of different degrees of HPTS trapping. The fs−ns experiments show that the proton-transfer reactions in these complexes happen in a large time window, spanning from 150 fs to ~1.2 ns, stemming from the heterogeneous nature of the system. The shortest component indicates a direct reaction in the robust complexes (involving the carboxylate groups of the amino acids), while the slowest one is due the slow dynamics of the biological water. We also found other time constants of the caged ROH* to form the RO^{-}* in; 3 to tens of ps, assigned to the reaction within "loose" complexes, and 130 ps and 1.2 ns due to the slow dynamics of the biological water molecules involved in the proton transfer.

The fs−ns anisotropy measurements confirm the robustness of HPTS:HSA complexes. Furthermore, the initial anisotropy ($r(0)$) value suggests that the protein ($r(0) = 0.33$) and the cyclodextrin ($r(0) = 0.28$) caging differently affects the mixing of the ^1L_a and ^1L_b states of the formed conjugated bases into these cavities. The difference is explained in terms of strong H-bonds and/or electrostatic interactions of the aminoacids with the sulfonate groups of the trapped dye affecting the electronic redistribution in the caged RO^{-}*, while these groups in the hydrophic pocket of CD are protected from the H-bonds with water molecules, contrary to the situation in water, where $r(0) = 0.385$.

■ ASSOCIATED CONTENT

Supporting Information. Additional information about the complexation between γ-CD and HPTS, time-correlated single-photon counting decays of HPTS in phosphate buffer and in the presence of HSA protein and short delay time windows. This material is available free of charge via the Internet at http://pubs.acs.org.

■ AUTHOR INFORMATION

Corresponding Author

*E-mail: Abderrazzak.Douhal@uclm.es. Fax: +34-925-268840. Phone: +34-925-265717.

■ ACKNOWLEDGMENT

This work was supported by the MICINN and EU through projects MAT2008-01609, UNCM08-1E-068, UNCM08-1E-050, and CYCLON Network (MRTN-CT-2008-Project 237962), respectively. B.C. thanks the MICINN for the Ramón y Cajal Contract.

■ REFERENCES

(1) Hynes, J. T., Klinman, J. P., Limbach, H.-H., Schowen, R. L., Eds. *Hydrogen-Transfer Reactions*, 1st ed.; Wiley-VCH: Weinheim, Germany, 2007; Vols. 1−4.

(2) Eigen, M. *Angew. Chem.* **1963**, *75*, 489.

(3) Eigen, M.; Kruse, W.; Maass, G.; de Maeyer, L. In *Progress in Reaction Kinetics*; Porter, G., Ed.; Pergamon: Oxford, 1964; Vol. 2, p 285.
(4) Weller, A. *Z. Phys. Chem.* **1957**, *13*, 335.
(5) Weller, A. *Z. Phys. Chem.* **1958**, *17*, 224.
(6) Weller, A. In *Progress in Reaction Kinetics*; Porter, G., Ed.; Pergamon Press: Oxford, 1961; Vol. 1, p 187.
(7) Douhal, A.; Lahmani, F.; Zewail, A. H. *Chem. Phys.* **1996**, *207*, 477.
(8) Douhal, A.; Kim, S. K.; Zewail, A. H. *Nature* **1995**, *378*, 260.
(9) Cox, M. J.; Timmer, R. L. A.; Bakker, H. J.; Park, S.; Agmon, N. *J. Phys. Chem. A* **2009**, *113*, 6599.
(10) Agmon, N. *J. Phys. Chem. A* **2005**, *109*, 13.
(11) Cohen, B.; Huppert, D.; Agmon, N. *J. Am. Chem. Soc.* **2000**, *122*, 9838.
(12) Cohen, B.; Huppert, D.; Agmon, N. *J. Phys. Chem. A* **2001**, *105*, 7165.
(13) Staib, A.; Borgis, D.; Hynes, J. T. *J. Chem. Phys.* **1995**, *102*, 2487.
(14) Borgis, D.; Hynes, J. T. *J. Phys. Chem.* **1996**, *100*, 1118.
(15) Ando, K.; Hynes, J. T. *J. Phys. Chem. B* **1997**, *101*, 10464.
(16) Pines, E.; Huppert, D. *Chem. Phys. Lett.* **1986**, *126*, 88.
(17) Agmon, N.; Pines, E.; Huppert, D. *J. Chem. Phys.* **1988**, *88*, 5631.
(18) Pines, E.; Huppert, D.; Agmon, N. *J. Chem. Phys.* **1988**, *88*, 5620.
(19) von Smoluchowski, M. *Z. Phys. Chem.* **1917**, *92*, 129.
(20) Collins, F. C.; Kimball, G. E. *J. Colloid Sci.* **1949**, *4*, 425.
(21) Krissinel, E. B.; Agmon, N. *J. Comput. Chem.* **1996**, *17*, 1085.
(22) Szabo, A. *J. Phys. Chem.* **1989**, *93*, 6929.
(23) Rice, S. A. *Diffusion-Limited Reactions*; Elsevier: Amsterdam, The Netherlands, 1985.
(24) Spry, D. B.; Goun, A.; Fayer, M. D. *J. Phys. Chem. A* **2007**, *111*, 230.
(25) Rini, M.; Magnes, B.-Z.; Pines, E.; Nibbering, E. T. J. *Science* **2003**, *301*, 349.
(26) Mohammed, O. F.; Pines, D.; Dreyer, J.; Pines, E.; Nibbering, E. T. J. *Science* **2005**, *310*, 83.
(27) Mohammed, O. F.; Pines, D.; Nibbering, E. T. J.; Pines, E. *Angew. Chem., Int. Ed.* **2007**, *46*, 1458.
(28) Mohammed, O. F.; Pines, D.; Pines, E.; Nibbering, E. T. J. *Chem. Phys.* **2007**, *341*, 240.
(29) Siwick, B. J.; Bakker, H. J. *J. Am. Chem. Soc.* **2007**, *129*, 13412.
(30) Cox, M. J.; Bakker, H. J. *J. Chem. Phys.* **2008**, *128*, 174501/1.
(31) Siwick, B. J.; Cox, M. J.; Bakker, H. J. *J. Phys. Chem. B* **2008**, *112*, 378.
(32) Cohen, B.; Huppert, D. *MCLC S&T, Sect. B: Nonlinear Opt.* **2000**, *24*, 191.
(33) Genosar, L.; Cohen, B.; Huppert, D. *J. Phys. Chem. A* **2000**, *104*, 6689.
(34) Tran-Thi, T. H.; Gustavsson, T.; Prayer, C.; Pommeret, S.; Hynes, J. T. *Chem. Phys. Lett.* **2000**, *329*, 421.
(35) Tran-Thi, T. H.; Prayer, C.; Millie, P.; Uznanski, P.; Hynes, J. T. *J. Phys. Chem. A* **2002**, *106*, 2244.
(36) Arnaut, L. G.; Formosinho, S. J. *J. Photochem. Photobiol., A* **1993**, *75*, 1.
(37) Spry, D. B.; Fayer, M. D. *J. Chem. Phys.* **2008**, *128*, 084508/1.
(38) Spry, D. B.; Fayer, M. D. *J. Phys. Chem. B* **2009**, *113*, 10210.
(39) Moilanen, D. E.; Spry, D. B.; Fayer, M. D. *Langmuir* **2008**, *24*, 3690.
(40) Spry, D. B.; Goun, A.; Glusac, K.; Moilanen, D. E.; Fayer, M. D. *J. Am. Chem. Soc.* **2007**, *129*, 8122.
(41) Roy, D.; Karmakar, R.; Mondal, S. K.; Sahu, K.; Bhattacharyya, K. *Chem. Phys. Lett.* **2004**, *399*, 147.
(42) Mondal, S. K.; Sahu, K.; Sen, P.; Roy, D.; Ghosh, S.; Bhattacharyya, K. *Chem. Phys. Lett.* **2005**, *412*, 228.
(43) Mondal, S. K.; Sahu, K.; Ghosh, S.; Sen, P.; Bhattacharyya, K. *J. Phys. Chem. A* **2006**, *110*, 13646.
(44) Ghosh, S.; Dey, S.; Mandal, U.; Adhikari, A.; Mondal, S. K.; Bhattacharyya, K. *J. Phys. Chem. B* **2007**, *111*, 13504.
(45) Mondal, T.; Das, A. K.; Sasmal, D. K.; Bhattacharyya, K. *J. Phys. Chem. B* **2010**, *114*, 13136.
(46) Sen Mojumdar, S.; Mondal, T.; Das, A. K.; Dey, S.; Bhattacharyya, K. *J. Chem. Phys.* **2010**, *132*, 194505/1.
(47) Gutman, M.; Huppert, D.; Nachliel, E. *Eur. J. Biochem.* **1982**, *121*, 637.
(48) Gepshtein, R.; Leiderman, P.; Huppert, D.; Project, E.; Nachliel, E.; Gutman, M. *J. Phys. Chem. B* **2006**, *110*, 26354.
(49) Hynes, J. T.; Tran-Thi, T.-H.; Granucci, G. *J. Photochem. Photobiol., A* **2002**, *154*, 3.
(50) Spry, D. B.; Goun, A.; Bell, C. B., III; Fayer, M. D. *J. Chem. Phys.* **2006**, *125*, 144514/1.
(51) Silverman, L. N.; Spry, D. B.; Boxer, S. G.; Fayer, M. D. *J. Phys. Chem. A* **2008**, *112*, 10244.
(52) Mohammed, O. F.; Dreyer, J.; Magnes, B.-Z.; Pines, E.; Nibbering, E. T. J. *ChemPhysChem* **2005**, *6*, 625.
(53) Peters, T., Jr. *All About Albumin: Biochemistry, Genetics, and Medical Applications*; Academic Press: San Diego, CA, 1995.
(54) He, X. M.; Carter, D. C. *Nature* **1992**, *358*, 209.
(55) Zhong, D.; Douhal, A.; Zewail, A. H. *Proc. Natl. Acad. Sci. U.S.A.* **2000**, *97*, 14056.
(56) Qiu, W.; Zhang, L.; Okobiah, O.; Yang, Y.; Wang, L.; Zhong, D.; Zewail, A. H. *J. Phys. Chem. B* **2006**, *110*, 10540.
(57) Organero, J. A.; Tormo, L.; Douhal, A. *Chem. Phys. Lett.* **2002**, *363*, 409.
(58) Gil, M.; Douhal, A. *Chem. Phys. Lett.* **2006**, *428*, 174.
(59) Goldberg, S. Y.; Pines, E.; Huppert, D. *Chem. Phys. Lett.* **1992**, *192*, 77.
(60) Pines, E.; Huppert, D. *J. Chem. Phys.* **1986**, *84*, 3576.
(61) Douhal, A. *Chem. Rev.* **2004**, *104*, 1955.
(62) Nandi, N.; Bhattacharyya, K.; Bagchi, B. *Chem. Rev.* **2000**, *100*, 2013.
(63) Friedman, R.; Nachliel, E.; Gutman, M. *J. Biol. Phys.* **2005**, *31*, 433.
(64) Friedman, R.; Nachliel, E.; Gutman, M. *Biophys. J.* **2005**, *89*, 768.
(65) Gutman, M.; Nachliel, E.; Friedman, R. *Biochim. Biophys. Acta, Bioenerg.* **2006**, *1757*, 931.
(66) Friedman, R. *Isr. J. Chem.* **2009**, *49*, 149.
(67) Patargias, G. N.; Harris, S. A.; Harding, J. H. *J. Chem. Phys.* **2010**, *132*, 235103.
(68) Schutz, C. N.; Warshel, A. *Proteins* **2001**, *44*, 400.
(69) Sham, Y. Y.; Muegge, I.; Warshel, A. *Biophys. J.* **1998**, *74*, 1744.
(70) Adamczyk, K.; Premont-Schwarz, M.; Pines, D.; Pines, E.; Nibbering, E. T. J. *Science* **2009**, *326*, 1690.
(71) Adamczyk, K.; Dreyer, J.; Pines, D.; Pines, E.; Nibbering, E. T. J. *Isr. J. Chem.* **2009**, *49*, 217.
(72) Yamasaki, K.; Miyoshi, T.; Maruyama, T.; Takadate, A.; Otagiri, M. *Biol. Pharm. Bull.* **1994**, *17*, 1656.
(73) Sudlow, G.; Birkett, D. J.; Wade, D. N. *Mol. Pharmacol.* **1975**, *11*, 824.
(74) Urien, S.; Nguyen, P.; Berlioz, S.; Bree, F.; Vacherot, F.; Tillement, J. P. *Biochem. J.* **1994**, *302*, 69.
(75) Moreno, F.; Cortijo, M.; Gonzalez-Jimenez, J. *Photochem. Photobiol.* **1999**, *69*, 8.
(76) Aki, H.; Yamamoto, M. *J. Pharm. Sci.* **1994**, *83*, 1712.
(77) Ojala, W. H.; Sudbeck, E. A.; Lu, L. K.; Richardson, T. I.; Lovrien, R. E.; Gleason, W. B. *J. Am. Chem. Soc.* **1996**, *118*, 2131.
(78) Douhal, A.; Sanz, M.; Tormo, L. *Proc. Natl. Acad. Sci. U.S.A.* **2005**, *102*, 18807.
(79) Rini, M.; Pines, D.; Magnes, B.-Z.; Pines, E.; Nibbering, E. T. J. *J. Chem. Phys.* **2004**, *121*, 9593.
(80) Wardell, M.; Wang, Z. M.; Ho, J. X.; Robert, J.; Ruker, F.; Ruble, J.; Carter, D. C. *Biochem. Biophys. Res. Commun.* **2002**, *291*, 813.
(81) Pal, S. K.; Zewail, A. H. *Chem. Rev.* **2004**, *104*, 2099.

(82) Tormo, L.; Organero, J. A.; Douhal, A. *J. Phys. Chem. B* **2005**, *109*, 17848.
(83) Castellano, F. N.; Dattelbaum, J. D.; Lakowicz, J. R. *Anal. Biochem.* **1998**, *255*, 165.
(84) Ferrer, M. L.; Duchowicz, R.; Carrasco, B.; Garcia de la Torre, J.; Acuña, A. U. *Biophys. J.* **2001**, *80*, 2422.